JOE: A Mobile, Inverted Pendulum

Felix Grasser, Aldo D'Arrigo, Silvio Colombi, *Member, IEEE*, and Alfred C. Rufer, *Senior Member, IEEE*

***Abstract*—The Industrial Electronics Laboratory at the Swiss Federal Institute of Technology, Lausanne, Switzerland, has built a prototype of a revolutionary two-wheeled vehicle. Due to its configuration with two coaxial wheels, each of which is coupled to a dc motor, the vehicle is able to do stationary U-turns. A control system, made up of two decoupled state-space controllers, pilots the motors so as to keep the system in equilibrium. See http://leiwww.epfl.ch/joe for a video demonstration of JOE.**

***Index Terms*—Digital signal processor, gyroscope, modeling, robotics, state-space control.**

I. Introduction

PICTURE the scene in a café somewhere in Lausanne, Switzerland. The members of the team of the "Industrial Electronics Laboratory" are having a drink or two when suddenly someone comes up with an idea: "Wouldn't it be fun to build a vehicle that balances its driver on two coaxial wheels? Some sort of an electronically controlled monocycle." It was based on that idea that we set out to create a truly mobile, autonomous inverted pendulum.

Even though the theoretical approach is not simple, simulation results have rapidly proven the feasibility of such a concept.

In order to reduce cost as well as danger for the test pilots, it was decided on building a scaled-down prototype carrying a weight instead of a driver.

The vehicle is composed of a chassis carrying a dc motor coupled to a planetary gearbox for each wheel, the digital signal processor (DSP) board used to implement the controller, the power amplifiers for the motors, the necessary sensors to measure the vehicle's states, the receiver for the radio control unit, as well as a vertical steel bar. The batteries are bolted onto the steel bar, their mass "simulating" a driver. The wheels of the vehicle are directly coupled to the output shaft of the gearboxes.

Fig. 1 shows the vehicle with its three degrees of freedom (3-DOF). It is able to rotate around the z axis (pitch), a movement described by the angle Θ_P and the corresponding angular velocity ω_P. The linear movement of the chassis is characterized by the position x_{RM} and the speed v_{RM}. Additionally, the vehicle can rotate around its vertical axis (yaw) with the associated angle δ and angular velocity $\dot{\delta}$. These six state-space variables fully describe the dynamics of the 3-DOF system.

Manuscript received November 18, 2000; revised July 16, 2001.

F. Grasser and A. C. Rufer are with the Industrial Electronics Laboratory, Swiss Federal Institute of Technology, 1015 Lausanne, Switzerland (e-mail: felix.grasser@epfl.ch; alfred.rufer@epfl.ch).

A. D'Arrigo was with the Industrial Electronics Laboratory, Swiss Federal Institute of Technology, 1015 Lausanne, Switzerland. He is now with Electrica S.r.l., 20127 Milan, Italy (e-mail: aldo.darrigo@tiscalinet.it).

S. Colombi is with the Industrial Electronics Laboratory, Swiss Federal Institute of Technology, 1015 Lausanne, Switzerland, and also with IMV Invertomatic Technology SA, 6595 Riazzino, Switzerland (e-mail: scolombi@imv.com).

Publisher Item Identifier S 0278-0046(02)00928-0.

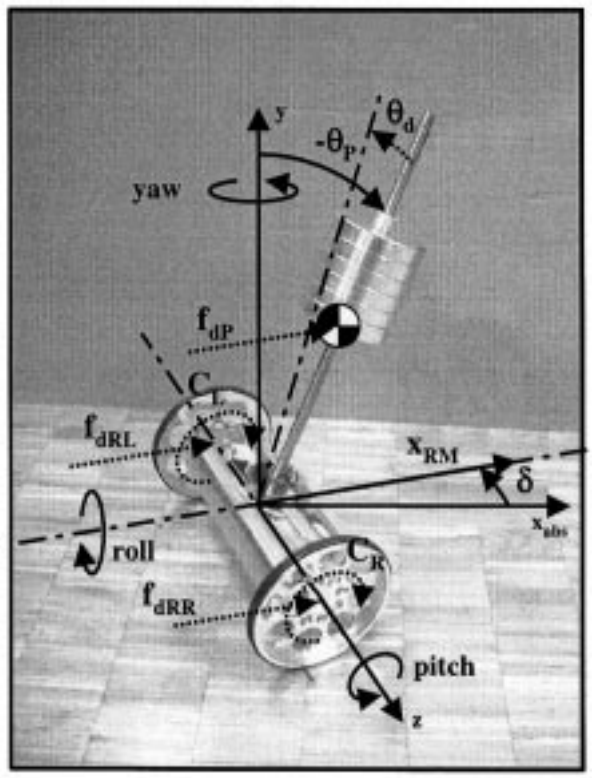

Fig. 1. Definition of state-space variables and disturbances.

Disturbances include forces applied to the center of gravity (CG) of the vehicle, f_{dP}, to the center of the left wheel, f_{dRL}, to the center of the right wheel, f_{dRR}, as well as a disturbance angle Θ_d. Θ_d describes a disturbance due to a change in location of the CG. On a full-sized vehicle (with the driver sitting on-board), this would typically be due to the driver moving on his seat.

The vehicle is controlled by applying a torque C_L and C_R to the corresponding wheels.

In order to successfully control the system, the state-space variables have to be quantified, either through direct measurement or an appropriate observer. x_{RM}, v_{RM}, δ, and $\dot{\delta}$ can be easily determined with the incremental encoders mounted on the two dc motors (provided Θ_P and ω_P are known). The angular velocity ω_P is measured by a rate gyroscope. Numerical integration [1], [2] of that signal calculates the associated pitch angle Θ_P.

The control system is based on two decoupled state-space controllers: one controlling the stability around the lateral axis (pitch) and a second one acting on the dynamics around the vertical axis (yaw). Each controller outputs a torque to be applied around its associated axis. A decoupling unit then translates these two signals into a torque to be applied to the left- and right-hand-side motors, respectively.

0278–0046/02$17.00 © 2002 IEEE

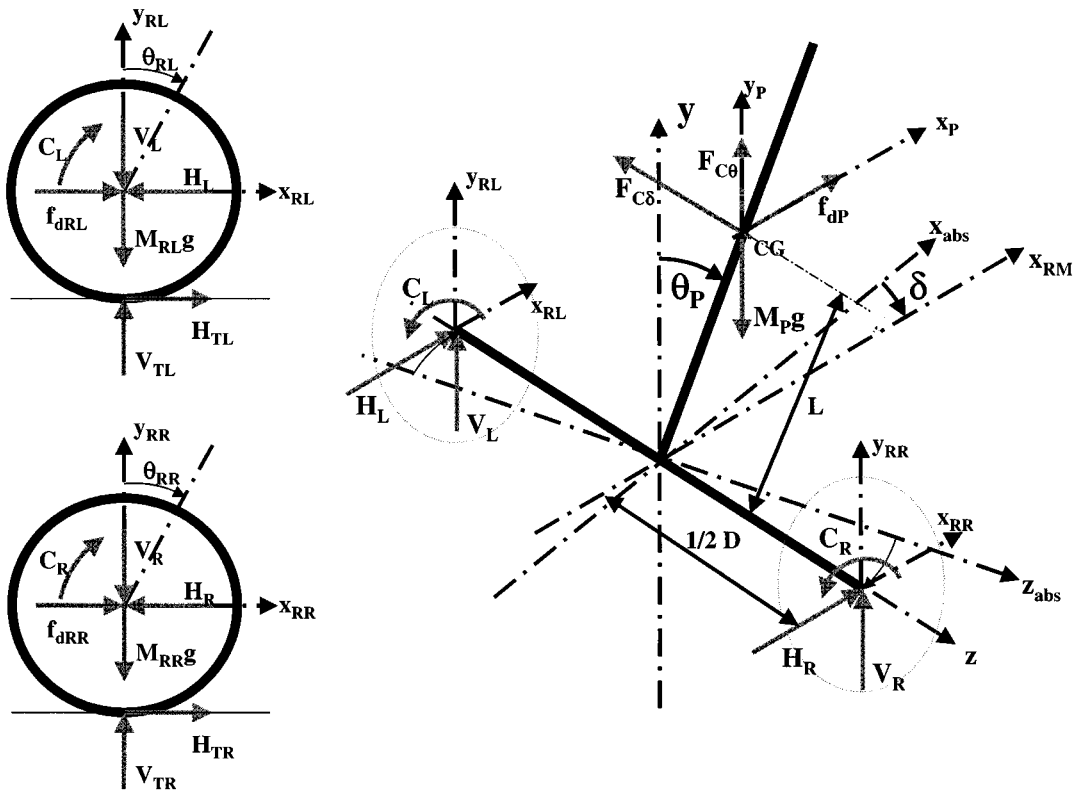

Fig. 2. Free body diagram of the vehicle.

The driver pilots the system with a radio control unit, transmitting the desired straight-line speed, v_{RMC} and the desired turning rate, $\dot{\delta}_C$ to the on-board control system.

II. Modeling

To develop an efficient control system for the vehicle, its dynamics have to be described by a mathematical model. This model [9] is based on the parameters characterizing the vehicle. Its behavior can be influenced by disturbances as well as by the motor torques.

The following variables have been chosen to describe the vehicle (see also Fig. 2):

- $\mathbf{J_{RL}}, \mathbf{J_{RR}}$—moment of inertia of the rotating masses with respect to the z axis (including the wheel, the rotational part of the gearbox, as well as the rotor of the dc motor);
- $\mathbf{M_{RL}}$, $\mathbf{M_{RR}}$—mass of the rotating masses connected to the left and right wheels;
- $\mathbf{J_{P\Theta}}$—moment of inertia of the chassis with respect to the z axis (Including the chassis, the nonrotating part of the gearbox, as well as the stator of the dc motor);
- $\mathbf{J_P}\delta$—moment of inertia of the chassis with respect to the y axis;
- $\mathbf{M_P}$—mass of the chassis;
- $\mathbf{R}$—radius of the wheels;
- $\mathbf{D}$—lateral distance between the contact patches of the wheels;
- $\mathbf{L}$—distance between the z axis and the CG of the chassis.

These parameters have been identified from a three-dimensional computer-aided design model of the system and were then subjected to an experimental verification [4], [8].

According to the definitions in Fig. 2, the following equations of motion can be defined (we will only give the equations for the left-hand wheel since the ones for the right-hand wheel are completely analogous):

$$\ddot{x}_{RL}M_{RL} = f_{dRL} - H_L + H_{TL} \tag{1}$$
$$\ddot{y}_{RL}M_{RL} = V_{TL} - M_{RL}g - V_L \tag{2}$$
$$\ddot{\Theta}_{RL}J_{RL} = C_L - H_{TL}R. \tag{3}$$

For the chassis,

$$\ddot{x}_P M_P = f_{dP} + H_R + H_L \tag{4}$$
$$\ddot{y}_P M_P = V_R + V_L - M_P g + F_{C\Theta} \tag{5}$$
$$\ddot{\Theta}_P J_{P\Theta} = (V_R + V_L)L\sin\Theta_P - (H_L + H_R)L\cos\Theta_P - (C_L + C_R) \tag{6}$$
$$\ddot{\delta}J_{P\delta} = (H_L - H_R)\frac{D}{2} \tag{7}$$

where H_L, H_R, H_{TL}, H_{TR}, V_L, V_R, V_{TL}, and V_{TR} represent reaction forces between the different free bodies.

It has to be noted that the moment of inertia $J_{P\delta}$ in (7) depends on the angular position Θ_P of the chassis. However, since we shall linearize the equations for small deviations of Θ_P around $\Theta_P = 0$ at a later stage, we will assume $J_{P\delta}$ to be constant at $J_{P\delta}\big|_{\Theta_P=0}$.

We shall also assume that the wheels of the vehicle always stay in contact with the ground and that there will be no slip at the wheel's contact patches. Therefore, there will be no movement in the z direction and no rotation about the x axis. Additionally, cornering forces are considered negligible.

Since the time constant of the electric motors (including current control loop) is small compared to the system's time constants, the motors dynamics have been neglected in the model.

Modifying (1)–(7) and then linearizing the result around the operating point ($x_{RM} = 0$; $\Theta_P = 0$ and $\delta = 0$) the system's state-space equations can be written in matrix form as

$$\begin{bmatrix} \dot{x}_{RM} \\ \dot{v}_{RM} \\ \dot{\Theta}_P \\ \dot{\omega}_P \\ \dot{\delta} \\ \ddot{\delta} \end{bmatrix} = \begin{bmatrix} 0 & 1 & 0 & 0 & 0 & 0 \\ 0 & 0 & A_{23} & 0 & 0 & 0 \\ 0 & 0 & 0 & 1 & 0 & 0 \\ 0 & 0 & A_{43} & 0 & 0 & 0 \\ 0 & 0 & 0 & 0 & 0 & 1 \\ 0 & 0 & 0 & 0 & 0 & 0 \end{bmatrix} \begin{bmatrix} x_{RM} \\ v_{RM} \\ \Theta_P \\ \omega_P \\ \delta \\ \dot{\delta} \end{bmatrix} + \begin{bmatrix} 0 & 0 & 0 & 0 & 0 \\ B_{21} & B_{22} & B_{23} & B_{24} & B_{25} \\ 0 & 0 & 0 & 0 & 0 \\ B_{41} & B_{42} & B_{43} & B_{44} & B_{45} \\ 0 & 0 & 0 & 0 & 0 \\ B_{61} & B_{62} & B_{63} & B_{64} & B_{65} \end{bmatrix} \begin{bmatrix} C_L \\ C_R \\ f_{dRL} \\ f_{dRR} \\ f_{dP} \end{bmatrix} \quad (8)$$

where A_{23}, A_{43}, B_{21}, B_{23}, B_{24}, B_{25}, B_{41}, B_{42}, B_{43}, B_{44}, B_{45}, B_{61}, B_{62}, B_{63}, B_{64}, and B_{65} are defined as a function of the vehicle's parameters.

With this state-space model, an appropriate control strategy can be developed to keep the vehicle in equilibrium and impose the desired speed and turning rate.

III. Control System Development

In this section, we shall look at the development of the control system, the desired performance, and how it has been achieved.

Equation (8) shows that there are five inputs to our system. Three of those, f_{dRL}, f_{dRR}, and f_{dP}, are disturbance forces and, therefore, cannot be used to control the system. However, the torques C_L and C_R applied to the left- and right-hand-side motors can be governed by the control system.

In order to impose the desired dynamics on the system, we would like to control the rotation around the z axis independently of the rotation around the y axis. This translates into having a controller producing an output signal corresponding to a torque C_δ around the vertical axis and another with an output torque C_Θ around the lateral axis.

To apply these torques on the system, we need a decoupling unit that transforms C_δ and C_Θ into the wheel torques C_L and C_R. From Fig. 3, we gather

$$\begin{bmatrix} C_L \\ C_R \end{bmatrix} = \begin{bmatrix} D_{11} & D_{12} \\ D_{21} & D_{22} \end{bmatrix} \begin{bmatrix} C_\Theta \\ C_\delta \end{bmatrix}. \quad (9)$$

For the equations to be more legible, we subsequently omit the disturbance forces when writing the state-space model of our system. Thus, we have

$$[\dot{\underline{x}}] = [\underline{A}][\underline{x}] + \begin{bmatrix} 0 & 0 \\ B_2 & B_2 \\ 0 & 0 \\ B_4 & B_4 \\ 0 & 0 \\ B_6 & -B_6 \end{bmatrix} \begin{bmatrix} C_L \\ C_R \end{bmatrix} \quad (10)$$

where $B_2 = B_{21} = B_{22}$, $B_4 = B_{41} = B_{42}$, and $B_6 = B_{61} = -B_{62}$.

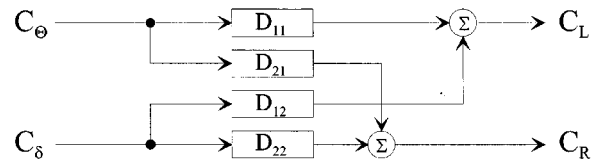

Fig. 3. Decoupling between the two subsystems.

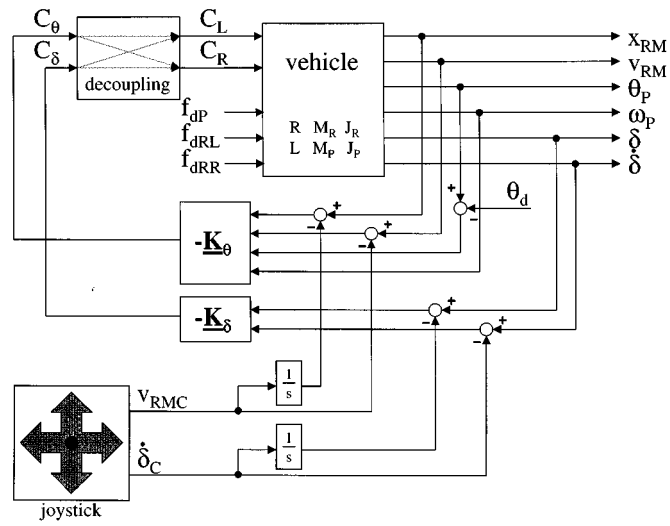

Fig. 4. Control system of the vehicle.

It can be seen from (10) that an input torque C_L, for example, will influence the system's dynamics around its vertical and lateral axis. In order to avoid this coupling [3], (10) has to be expressed as follows:

$$[\dot{\underline{x}}] = [\underline{A}][\underline{x}] + \begin{bmatrix} 0 & 0 \\ B_a & 0 \\ 0 & 0 \\ B_b & 0 \\ 0 & 0 \\ 0 & B_c \end{bmatrix} \begin{bmatrix} C_\Theta \\ C_\delta \end{bmatrix}. \quad (11)$$

Substituting (9) into (10) and then equating the result to (11) yields

$$\begin{bmatrix} 0 & 0 \\ B_2 & B_2 \\ 0 & 0 \\ B_4 & B_4 \\ 0 & 0 \\ B_6 & -B_6 \end{bmatrix} \begin{bmatrix} D_{11} & D_{12} \\ D_{21} & D_{22} \end{bmatrix} = \begin{bmatrix} 0 & 0 \\ B_a & 0 \\ 0 & 0 \\ B_b & 0 \\ 0 & 0 \\ 0 & B_c \end{bmatrix}. \quad (12)$$

$[D]$ can now be determined using (12). One of its elements can be chosen freely. Choosing $D_{11} = 0.5$ translates into

$$[\underline{D}] = \begin{bmatrix} 0.5 & 0.5 \\ 0.5 & -0.5 \end{bmatrix}. \quad (13)$$

Solving for B_a, B_b, and B_c gives

$$\begin{aligned} B_a &= B_2 \\ B_b &= B_4 \\ B_c &= B_6. \end{aligned} \quad (14)$$

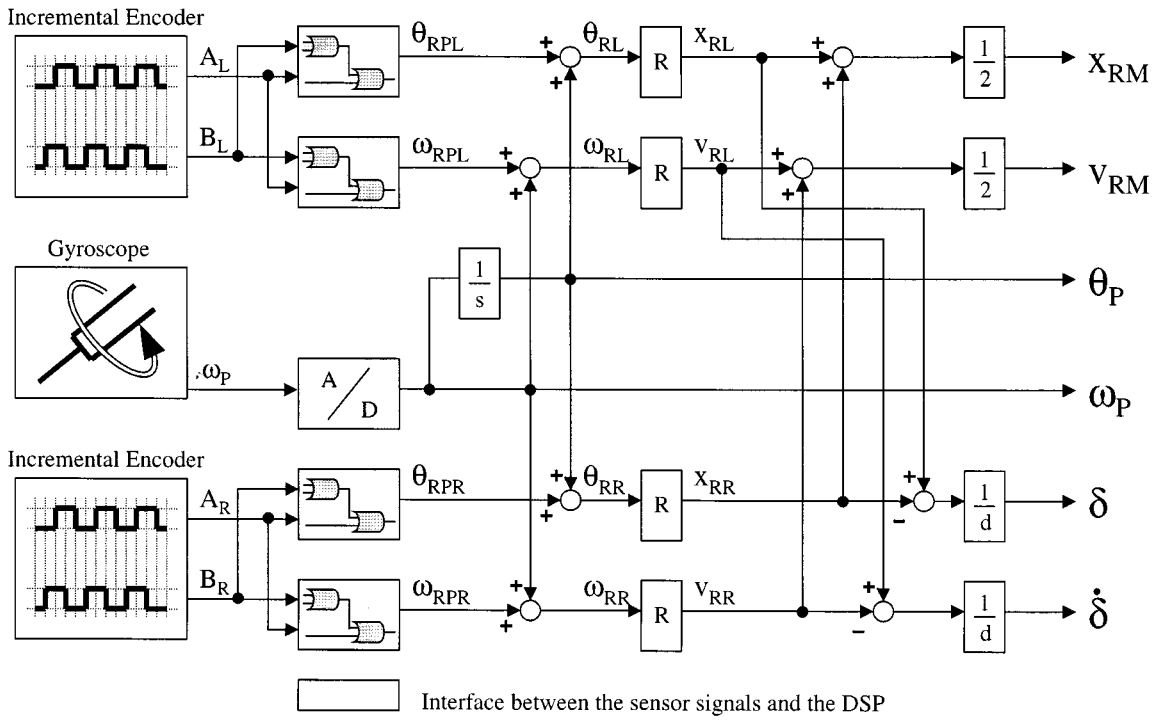

Fig. 5. Sensor signal processing.

The state-space equations for the vehicle can now be written as two different systems: 1) a system "pendulum" describing the rotation about the z axis and 2) a system "rotation" modeling the rotation about the y axis. For the "pendulum" we have

$$\begin{bmatrix} \dot{x}_{RM} \\ \ddot{x}_{RM} \\ \dot{\Theta}_P \\ \ddot{\Theta}_P \end{bmatrix} = \begin{bmatrix} 0 & 1 & 0 & 0 \\ 0 & 0 & A_{23} & 0 \\ 0 & 0 & 0 & 1 \\ 0 & 0 & A_{43} & 0 \end{bmatrix} \begin{bmatrix} x_{RM} \\ \dot{x}_{RM} \\ \Theta_P \\ \dot{\Theta}_P \end{bmatrix} + \begin{bmatrix} 0 \\ B_2 \\ 0 \\ B_4 \end{bmatrix} [C_\Theta] \tag{15}$$

and for the "rotation"

$$\begin{bmatrix} \dot{\delta} \\ \ddot{\delta} \end{bmatrix} = \begin{bmatrix} 0 & 1 \\ 0 & 0 \end{bmatrix} \begin{bmatrix} \delta \\ \dot{\delta} \end{bmatrix} + \begin{bmatrix} 0 \\ B_6 \end{bmatrix} [C_\delta]. \tag{16}$$

We are now able to design an independent controller for each of these subsystems with the possibility of assigning different dynamics to each of them.

The design of the state-space controllers [3] is straightforward and will not be presented here. We shall, however, come back to the pole placement issue in Section V when commenting on the achieved closed-loop dynamics.

The user will be able to pilot the system by imposing the straight-line speed v_{RMC} of the vehicle as well as its turning rate $\dot{\delta}_C$ around the vertical axis (Fig. 4).

IV. Control System Implementation

In this section, we look at the implementation of the two controllers. We present the chosen sensors as well as the problems experienced during the setup of the system.

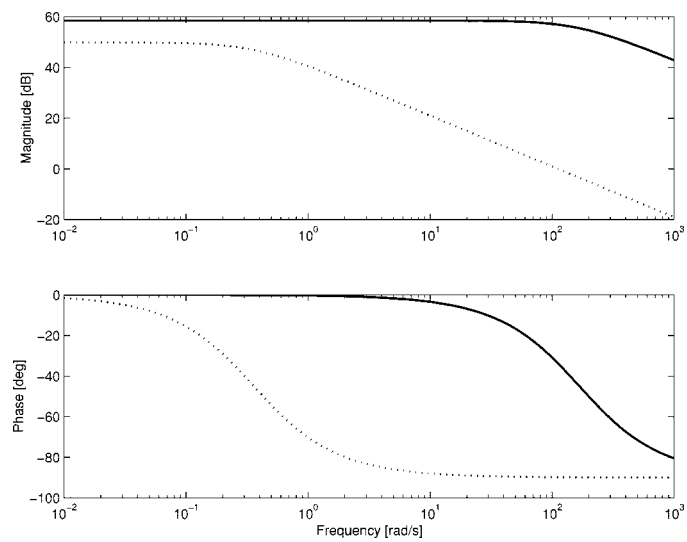

Fig. 6. Frequency response of the motor (solid line) and the motor with gearbox and wheel attached (dotted line).

A. Controller Hardware

The controller has been implemented on a DSP board developed at the Industrial Electronics Laboratory, Swiss Federal Institute of Technology, Lausanne, Switzerland, and distributed by CHS-Engineering (www.chs-eng.ch). It is composed of a Sharc floating-point DSP, a XILINX field-programmable gate array (FPGA), four 10-bit D/A converters, as well as 14 12-bit A/D converters [7]. Dedicated software enables the user to program the board and get readouts of all the variables while the system is running.

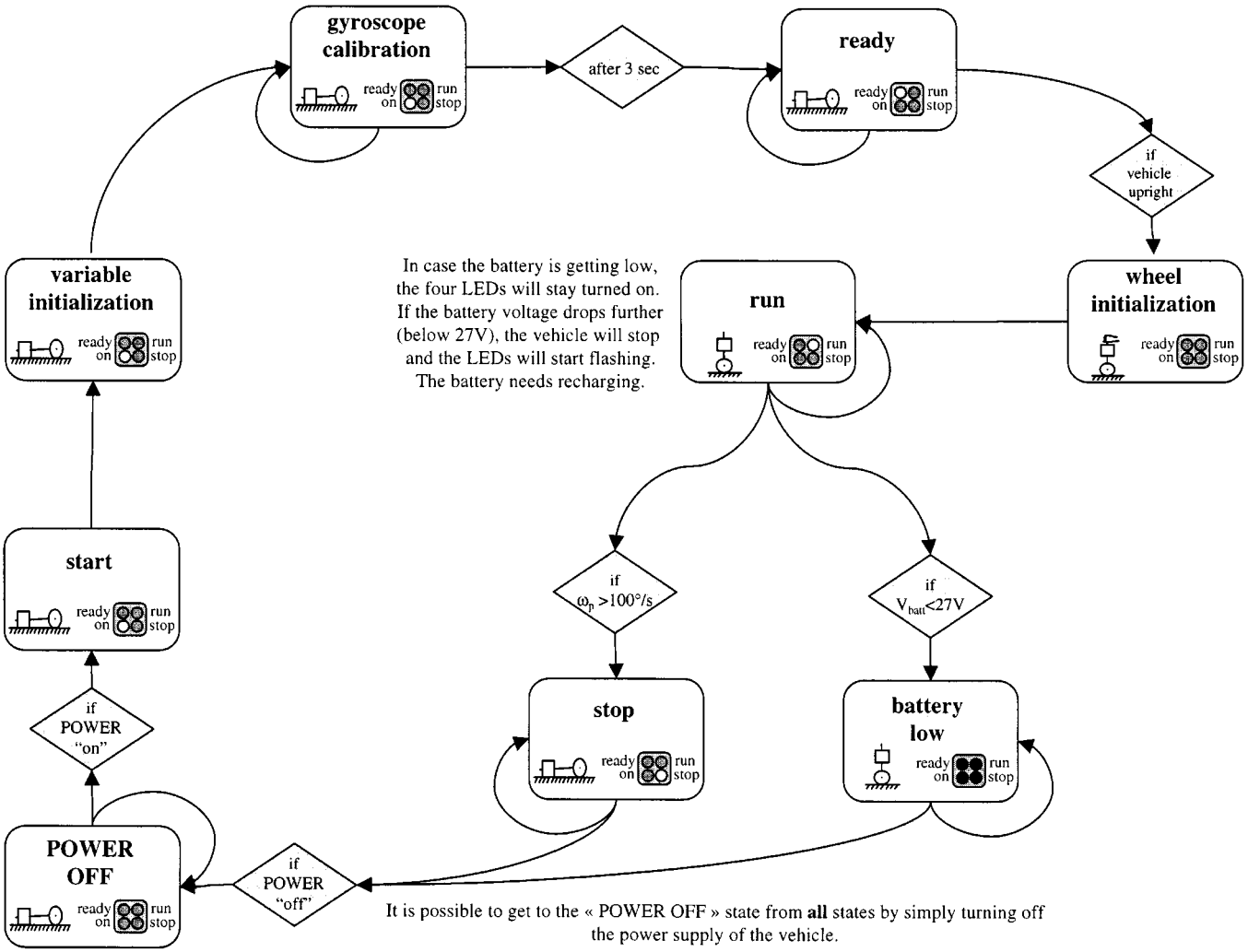

Fig. 7. Flowchart of the control system's states.

B. State Measurements

A gyroscope as well as two incremental encoders mounted on each dc motor measure the states of the vehicle. The processing of their output signals is shown in Fig. 5.

The incremental encoders are connected to the FPGA circuit where their signals are decoded [5] to yield information about the angle and angular velocity between the motor's rotor (i.e., the wheels) and stator (i.e., the chassis). With the angle and angular velocity of the chassis with respect to its lateral axis known (information obtained from the gyroscope), angular position and speed of the wheels can be transformed into straight-line speed and position of the chassis as well as its angular position and speed about the vertical axis.

As mentioned before, the pitch rate is determined by a solid-state gyroscope mounted on the vehicle and connected to an A/D converter. The corresponding pitch angle is then obtained by numerical integration of the pitch rate.

Such an integration of a measured pitch rate is sensitive to drift problems [1]. This phenomenon can be described by a ramp-shaped disturbance angle applied to the system. It can be shown that the control system is able to reject such a disturbance. It will, in fact, be rejected by compensation with the vehicle's position, i.e., the vehicle will slowly move forward (or backward) in order to catch the imaginary "fall."

C. Backlash

The use of a planetary gearbox introduces backlash between the wheels and the motors. Unfortunately, this nonlinearity directly affects our measurements [6] since the incremental encoders are mounted on the motors and not on the wheels.

When the direction of rotation is reversed, the motors will, therefore, briefly run with no load. Due to the much lower moment of inertia of the motor without gearbox, wheel, and load, the measured speeds will be high even though the wheel has not yet moved. The controller will try to counteract those high velocities by applying a torque in the other direction.

Apart from emitting an unpleasant noise, the resulting limit cycles will damage the gearbox and trigger mechanical resonances in the vehicle.

Knowing that the dynamics of the motor alone and the motor with gearbox and wheel attached are very different, it should be possible to design a low-pass filter eliminating any high-frequency speed measurements that can only occur in the "backlash zone."

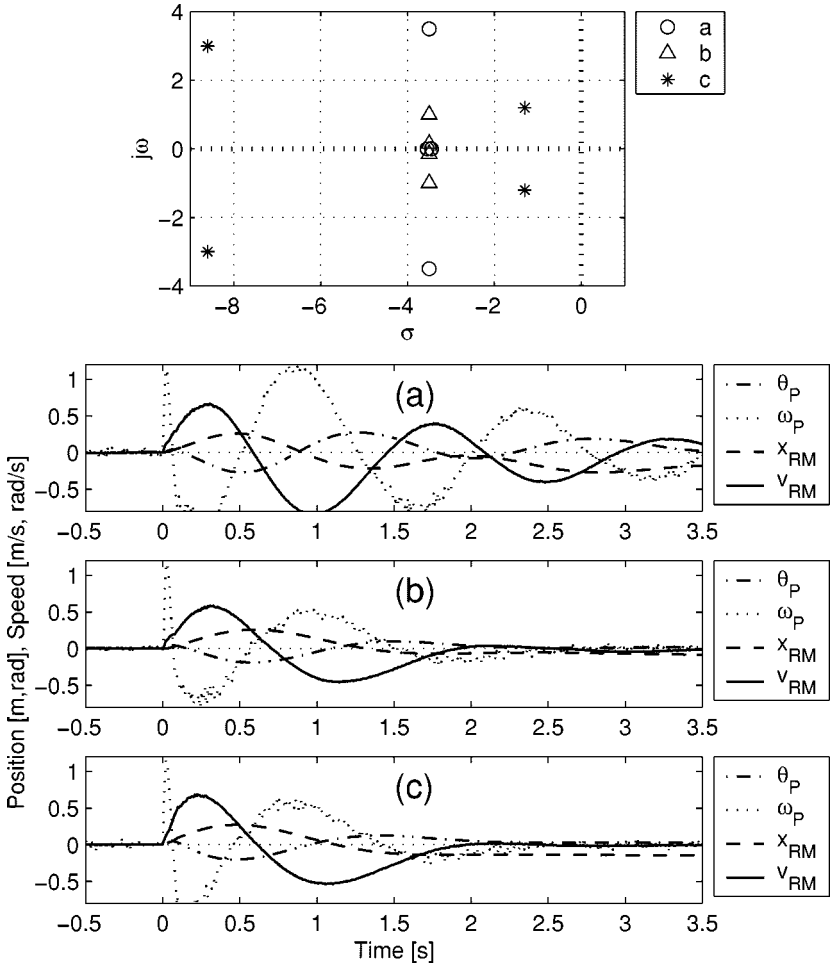

Fig. 8. Pole placement of the "pendulum" system and associated response to an impulse disturbance force (energy transmitted ≈ 1.2 J) applied to the pendulum.

A simple first-order model has proven sufficient to show the differences between the motor dynamics with and without gearbox and wheel.

According to the results shown in Fig. 6, we designed a first-order filter with a cutoff frequency of 10 rad/s preventing the speed measurements being affected by the gearbox play. Backlash, of course, still affects the system's dynamics, but its worst effects have been eliminated by filtering the speed measurements.

D. Control Interface

The control interface has been designed to be simple to use. It consists of a power-on switch mounted on the vehicle as well as a radio control unit with an emergency switch and two proportional levers.

When turned on, the control system will calibrate the sensors (Fig. 7). Once the "ready" light has come on, the user can simply lift the vehicle up. The control system will automatically switch to the "run" mode as soon as the vehicle is in an upright position. The vehicle can then be piloted by imposing a straight-line speed as well as a yaw rate on the proportional levers of the radio control unit.

In case the pitch rate is higher than about 100°/s (gyroscope limitation), the control system will automatically be switched off since we are no longer able to measure and feed back the vehicle's dynamics.

The battery voltage is permanently monitored by the control system. A couple of minutes prior to their being completely discharged, the four LEDs on the vehicle will stay turned on to signal a low state of charge. As soon as the batteries reach their minimal voltage, the LEDs will start flashing and the control system will no longer accept the pilot's inputs.

V. Driving the Results

JOE measures 65 cm in height and weighs about 12 kg; it can reach a maximum speed of 1.5 m/s. It is capable of climbing inclines up to 30° (depending on the actual coefficient of friction). On its 32-V 1.8-Ah battery, it has an autonomy of roughly one hour's driving time.

System performance (i.e., reaction to disturbance forces, tracking of driver input, etc.) is driven by the pole placement. In order to maximize JOE's performance, controllers with different pole placements have been tested.

For a chosen pole placement, the controller's gains were calculated and implemented on the DSP board. JOE was then tested with that controller configuration and the response recorded by the control system. Some of these responses are shown in Figs. 8 and 9.

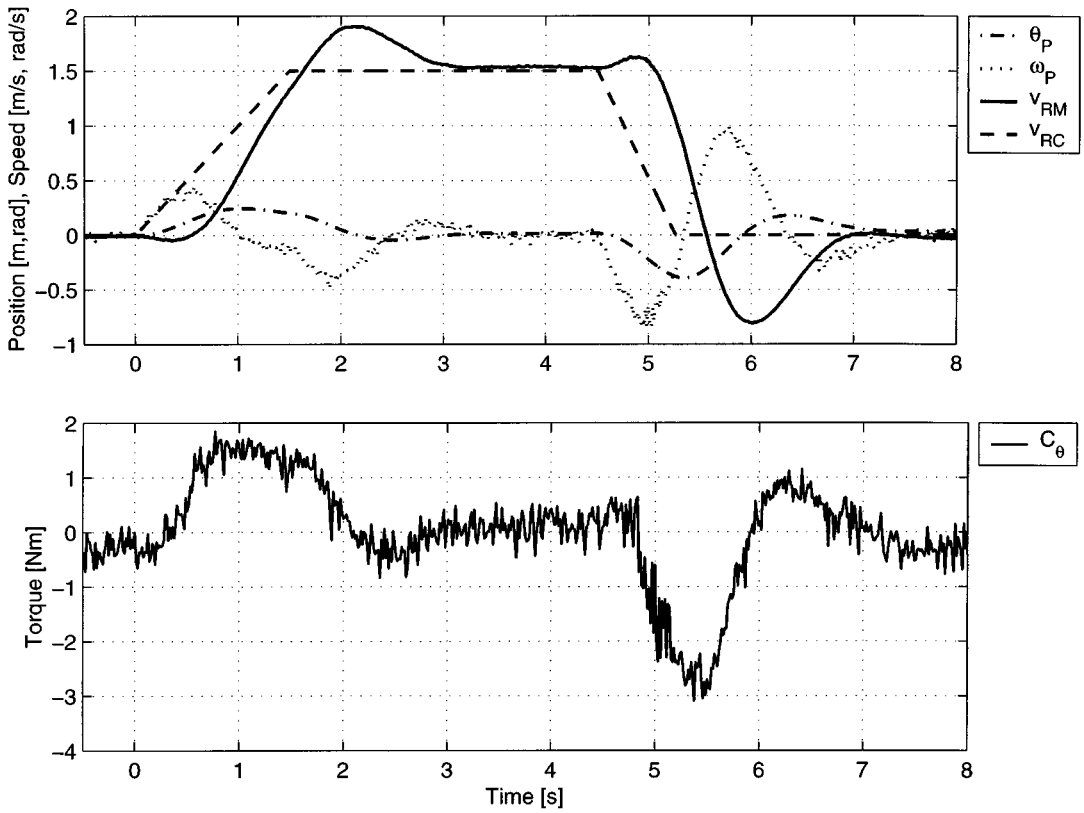

Fig. 9. Reaction to a ramp-shaped speed input.

The pole placement in Fig. 8(a) has been chosen as a starting point. Such a configuration yields an unsatisfactory behavior with badly damped oscillations. Increasing the damping ratio further (Fig. 8(b)) improves matters significantly.

We found that the system can be made to behave even better by placing the poles as shown in Fig. 8(c). Two very fast poles with a high damping factor are combined with two slower ones with a medium damping factor.

Increasing performance with the pole placement chosen can be achieved by moving the poles further to the left, thus making the system faster. Backlash (limit cycles) as well the maximum torque that can be transmitted to the ground (grip) prevent us from moving the poles past a certain limit. The placement shown in Fig. 8(c) represents the solution retained.

The authors think that an adaptive pole placement (depending on the system's state) would enable further improvements.

Fig. 9 shows the system's response to a velocity ramp input. Note that the maximum acceleration possible is lower than the maximum deceleration. Due to the motor's speed–current characteristics, a high torque cannot be obtained when operating at high speeds. However, this is exactly what is necessary to get the vehicle back into an upright position at the end of the acceleration phase. Deceleration demands maximum torque at low speeds—a steeper ramp is, therefore, possible.

Fig. 10. JOE.

VI. Conclusions

This paper has presented a mobile, inverted pendulum (Fig. 10). The control system used to guarantee stability of the system is based on two state-space controllers, interfaced via a decoupling unit to the two dc motors driving the wheels.

We have shown the performance of the system, its ability to reject force and angular disturbances, as well as its capability of tracking a pilot's driving inputs.

A control system varying the pole placement in real time depending on the states and inputs of the system has the potential to further increase JOE's performance. Such an adaptive controller could typically be based on fuzzy logic criteria.

ACKNOWLEDGMENT

The authors would like to express their thanks to everybody at the Industrial Electronics Laboratory at EPFL for their creative suggestions and precious help with any problems that arose during our work. F. Grasser would like to specially thank J.-M. Meyer for his priceless support and help during the whole project.

REFERENCES

[1] D. H. Titterton and J. L. Weston, *Strapdown Inertial Navigation Technology*. Stevenage, U.K.: Peregrinus, 1997.
[2] J. H. Mathews, *Numerical Methods for Mathematics, Science and Engineering*. Englewood Cliffs, NJ: Prentice-Hall, 1992.
[3] D. Gillet, "Commande avancée II—Notes de cours," EPFL, Lausanne, Switzerland, 1998.
[4] R. Longchamp, *Commande Numérique de Systèmes Dynamiques*. Lausanne, Switzerland: PPUR, 1995.
[5] H. Bühler, "Mecatronique," Laboratoire d'Électronique Industrielle, EPFL, Lausanne, Switzerland, 1992.
[6] S. Colombi, "Mecatronique—Notes de Cours," Laboratoire d'Électronique Industrielle, EPFL, Lausanne, Switzerland, 1998.
[7] M. Nicollerat and M. Montemari, *Functional Description of the David Board*. Martigny, Switzerland: CHS-Engineering, 1998.
[8] W. F. Riley and L. D. Sturges, *Engineering Mechanics: Dynamics*. New York: Wiley, 1996.
[9] A. D'Arrigo, "Veicolo elettrico sperimentale a due ruote parallele coassiali indipendenti," Thesi di laurea, EPFL/Politecnico di Milano, Lausanne, Switzerland/Milan, Italy, 1997.

Felix Grasser was born in Lucerne, Switzerland, in 1974. He received the Master's degree in mechanical engineering from the Swiss Federal Institute of Technology (EPFL), Lausanne, Switzerland, in 2000.

He is currently a Research Assistant in the Industrial Electronics Laboratory, EPFL.

Aldo D'Arrigo was born in Milan, Italy, in 1973. He received the Degree in electrical engineering from the Politecnico di Milano, Milan, Italy.

After completing his "Thesi di laurea" at the Swiss Federal Institute of Technology (EPFL), Lausanne, Switzerland, he was involved in different projects at EPFL and in Loughborough, U.K. In 1999, he joined Electrica S.r.l., Milan, Italy, where he is working in the field of thermal electric motor protection.

Silvio Colombi received the M.Sc. and Ph.D. degrees in electrical engineering from the Swiss Federal Institute of Technology (EPFL), Lausanne, Switzerland, in 1983 and 1987, respectively.

He was with the Joint European Torus, Abingdon, U.K., working on teleoperation problems in 1990 as an Associate Staff Member and during 1993–1994 as a TeleMan Fellow. As a Scientific Associate at EPFL, he worked on and led numerous industrial and research projects. He has negotiated and carried out several European projects and served as an independent consultant to industry. At present, he is responsible for the development of new technologies at IMV Invertomatic Technology, Locarno, Switzerland, and a Lecturer in mechatronics at EPFL. He is the holder of a number of industrial patents and the author of more than 30 technical papers dealing with modeling, control, mechatronics, and industrial electronics.

Alfred C. Rufer (SM'02) was born in Diessbach, Switzerland, in 1951. He received the Master's degree from the Swiss Federal Institute of Technology (EPFL), Lausanne, Switzerland, in 1976.

In 1978, he joined ABB, Turgi, Switzerland, where he worked in the fields of power electronics and control, including high-power variable-frequency converters for drives. In 1985, he was a Group Leader for power electronics development at ABB. In 1993, he became an Assistant Professor at EPFL. Since 1996, he has been a Professor and Head of the Industrial Electronics Laboratory, EPFL. He is the holder of several patents and is the author of a number of publications on modulation and control methods and power electronics.